Journal of Thermal Analysis and Calorimetry, Vol. 80 (2005) 71–75

THERMAL DEHYDRATION OF DIPOTASSIUM TETRABORATE TETRAHYDRATE AND CRYSTALLIZATION OF AMORPHOUS DEHYDRATION PRODUCT

*N. Koga**, *T. Utsuoka and H. Tanaka*

Chemistry Laboratory, Graduate School of Education, Hiroshima University, 1-1-1 Kagamiyama, Higashi-Hiroshima 739-8524, Japan

As one of the typical examples of producing an amorphous dehydration product, the thermal dehydration process of $K_2B_4O_7{\cdot}4H_2O$ was subjected to thermoanalytical and morphological studies. An anhydrous glass was formed via three distinguished dehydration stages. The overall thermal dehydration process was characterized as a self-induced sol–gel process to form anhydrous glass. The as produced anhydrous glass exhibited glass transition at around 700 K and subsequently crystallized via two consecutive exothermic peaks at around 770 and 900 K. The final crystallization product, triclinic $K_2B_4O_7$, melted at 1072 K.

Keywords: *crystallization, dipotassium tetraborate tetrahydrate, glass formation, sol–gel process, thermal dehydration*

Introduction

Although a type of thermal dehydration of inorganic hydrates which produce amorphous anhydrates is an interesting process accompanied by various physico-chemical events such as pre-melting and gelation [1], details of the formation mechanism of the amorphous anhydrates have not been clarified as yet [2, 3]. The thermal dehydration of alkaline and alkaline-earth metal borate hydrates can be classified into such a process producing amorphous anhydrates [4–6]. The present authors reported the kinetics and mechanism of the thermal dehydration of $Li_2B_4O_7{\cdot}3H_2O$ [7] and crystallization behavior of the amorphous product through comparison with that of melt-quenched glass of the corresponding composition [8, 9].

In the present study, the thermal dehydration process of $K_2B_4O_7{\cdot}4H_2O$ and the crystallization process of the amorphous product were subjected to thermoanalytical and morphological studies in order to clarify the characteristics of the physico-chemical events occurring in such a type of thermal dehydration processes. The thermal behavior of $K_2B_4O_7{\cdot}4H_2O$ including thermal dehydration, crystallization of the amorphous product and melting of the crystallized anhydrate were traced by TG-DTA and high temperature powder X-ray diffractometry (XRD) under various reaction conditions. The crystallization process of the amorphous dehydration product was followed by DSC. The morphological changes of the sample at various reaction stages were observed with a scanning electron microscope (SEM). Through such a systematic investigation on the thermal dehydration of $K_2B_4O_7{\cdot}4H_2O$, the thermal dehydration process which produces an amorphous dehydration product is characterized as one of the cases mentioned above.

Experimental

Reagent grade dipotassium tetraborate tetrahydrate (Sigma Aldrich Japan) was sieved to various fractions of particle size. The sieve fractions of –32+48, –100+170 and –200+280 meshes were used as the sample.

The sample (ca. 10.0 mg) weighed on a platinum pan (5 mm in diameter and 2.5 mm in height) were subjected to TG-DTA measurements using an instrument of ULVAC TGD9600 with an infrared image furnace. TG-DTA curves were recorded on heating from room temperature to 1100 K at various heating rates under flowing N_2 (80 mL min^{-1}).

Phase changes during heating were traced by a powder X-ray diffractometer (Rigaku RINT2200V) equipped with a programmable heating chamber using a monochromed CuK_α radiation (40 kV, 20 mA). Surface textures of the sample at selected typical reaction stages were observed by a SEM (JEOL JSM-T20) after lightly coating the surface by Au evaporation. Crystallization processes of the amorphous dehydration product were traced by DSC using an instrument of ULVAC DSC9400.

* Author for correspondence: nkoga@hiroshima-u.ac.jp

1388–6150/$20.00

Akadémiai Kiadó, Budapest, Hungary
Springer, Dordrecht, The Netherlands

Results and discussion

Figure 1 shows typical TG-DTA curves for $K_2B_4O_7{\cdot}4H_2O$ of different fractions of particle sizes. The thermal dehydration takes place in a wide temperature range from 400 to 750 K, indicating the rapid mass loss at the first half and decelerating mass loss at the second half of the dehydration. The averaged value of total mass loss, 23.8±0.3%, was in good agreement with the theoretical value (23.59%) calculated by assuming the following dehydration reaction: $K_2B_4O_7{\cdot}4H_2O \rightarrow K_2B_4O_7+4H_2O$. The endothermic DTA peak for the second half of the dehydration is detectable only for the sample with the larger particle sizes. After completing the dehydration, two distinguished exothermic DTA peaks can be observed at around 770 and 900 K. The second exothermic DTA peaks are more distinguished with decreasing the particle size of the sample. Irrespective of the particle size, abrupt endothermic peaks were observed at 1072 K, which is assigned to melting of $K_2B_4O_7$.

Further detailed reaction behaviors of the thermal dehydration and crystallization of dehydration product were investigated using the sample of –100+170 mesh sieve fraction. Figure 2 shows the changes of XRD patterns during heating the sample at a heating rate of 10 K min^{-1} under flowing N_2 (100 mL min^{1}). The original XRD pattern of $K_2B_4O_7{\cdot}4H_2O$ disappears during the rapid mass loss at the first half of the dehydration, producing an amorphous phase. The crystallization of the amorphous anhydrate was observed on the XRD pattern measured at 773 K, which resulted just after the first DTA exothermic peak appeared, as shown in Fig. 1. The crystal structure of the crystallized phase cannot be identified at present. The second DTA exothermic peak is interpreted as a structural phase transition due to apparent change in the XRD patterns observed between 873 and 973 K. The XRD pattern of the high temperature phase corresponds to the triclinic $K_2B_4O_7$ [10]. Within our knowledge, existence of the intermediate phase during the crystallization of $K_2B_4O_7$ glass has not been reported earlier. Determination of the crystallographic structure of the new phase is left for the future task to understand the detailed mechanism of the crystallization of amorphous dehydration product.

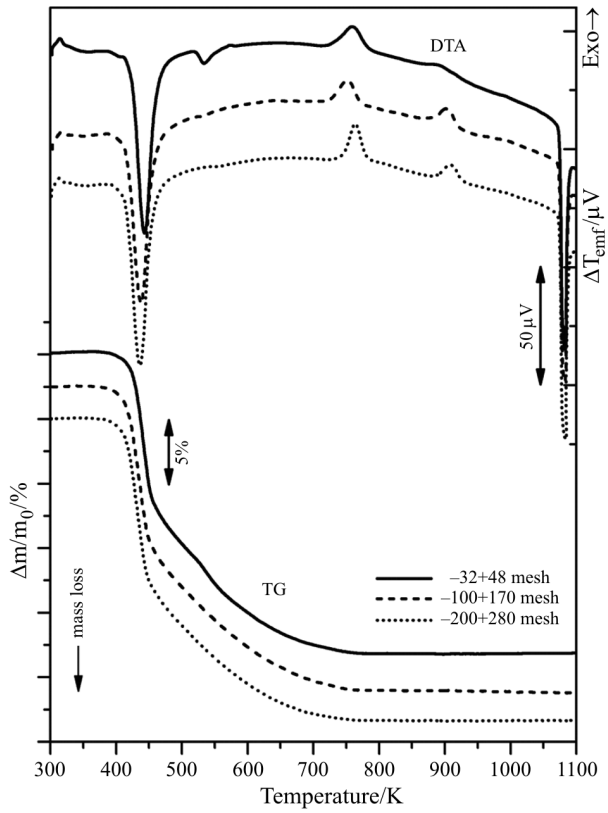

Fig. 1 Typical TG and DTA curves for the thermal dehydration of $K_2B_4O_7{\cdot}4H_2O$ with different sieve fractions

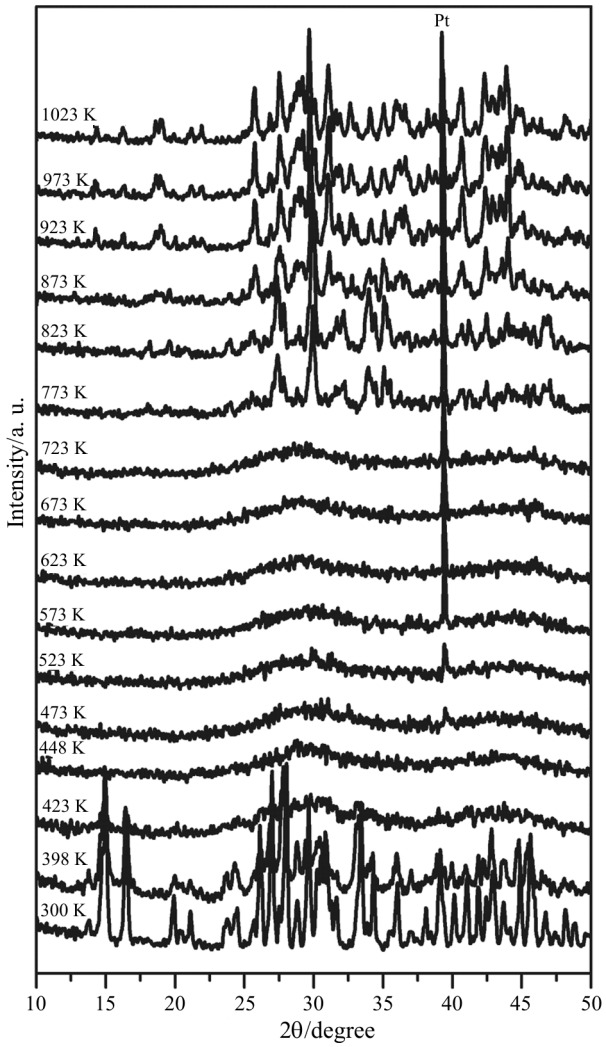

Fig. 2 Changes of XRD patterns during heating the sample at a heating rate of 10 K min^{-1}

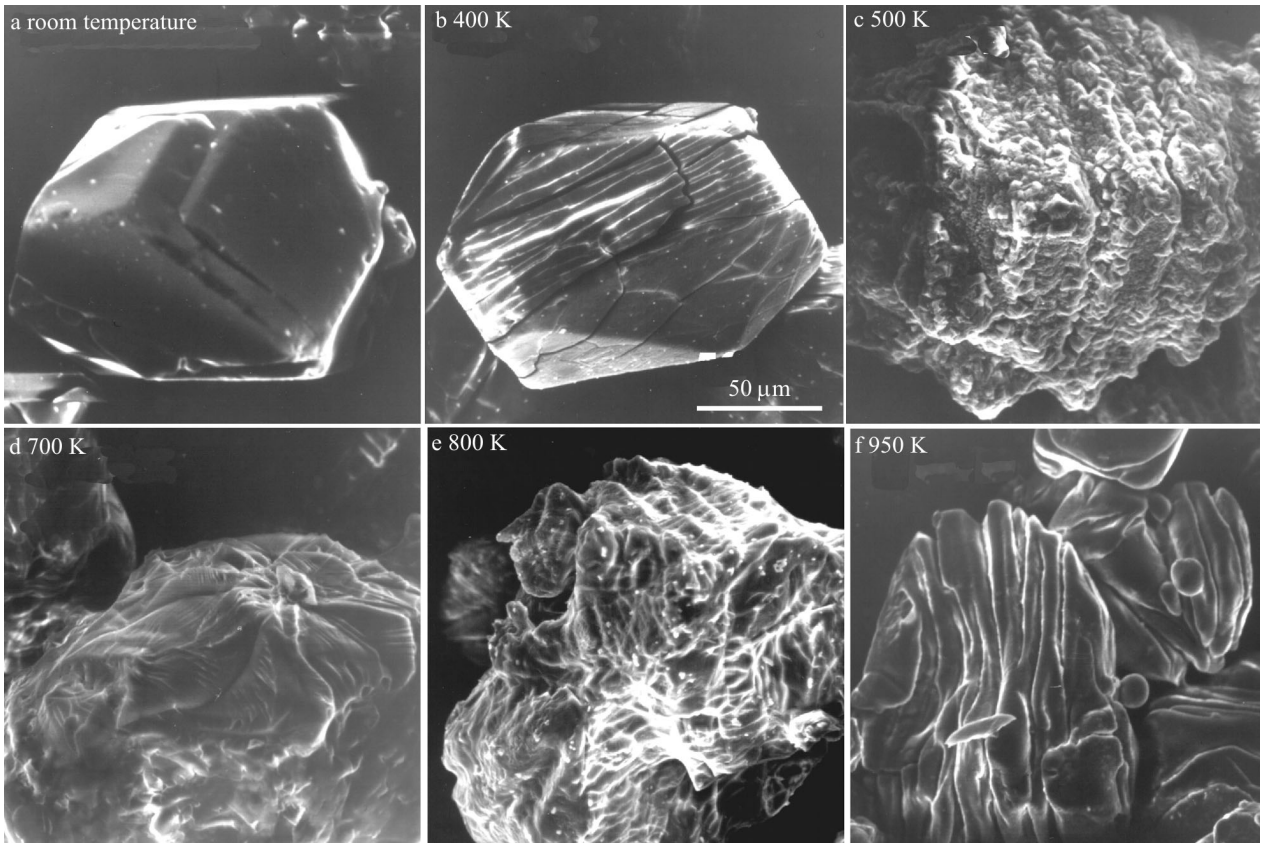

Fig. 3 Typical SEM images of the sample at selected reaction stages

Typical SEM photographs of the sample heated to various reaction steps were shown in Fig. 3. Just after initiation of the dehydration, cracks form on the surface, Fig. 3b. The rapid mass loss process at the first half dehydration produces aggregated fine powders on the surface, Fig. 3c. At this stage, the original crystal structure of the reactant has already been destructed, as illustrated by an amorphous phase detected by the XRD pattern. It is assumed that gel powders of hydrated $K_2B_4O_7$ are formed in the bulk of the sample particles through the first half of dehydration. The formation process of the gel powders may be explained by a possible sol–gel process originated from condensation of water vapor evolved by the thermal dehydration and the dissolution of the reactant solid into the condensed water. In that case, the rapid mass loss process is interpreted as evolution of water vapor from the sol solution or wet gel.

The second half of the dehydration process characterized by a gradual mass loss in a wider temperature region is explained by the dehydration from the gel powders of the hydrated $K_2B_4O_7$ without crystallization. As can be seen in Fig. 3d, surface of the completely dehydrated product shows smooth and glassy. The reformation of surface during the dehydration from the gel powder suggests the sintering of the gel powders. Figure 4 shows a typical DSC curve for the amorphous dehydration product. Prior to two distinguished exothermic peaks, an apparent endothermic shift due to glass transition is observed at around 700 K. The existence of the glass transition indicates that, during the process of the thermal dehydration of $K_2B_4O_7{\cdot}4H_2O$, a glass formation through sol–gel process [11] proceeds by an interaction of self-generated water vapor and the reactant solid.

Figure 5 shows the influence of heating rate on the TG and DTG curves for the thermal dehydration of

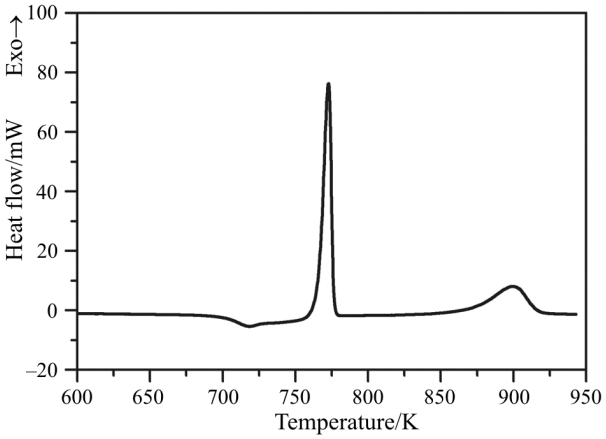

Fig. 4 A typical DSC curve for the amorphous dehydration product

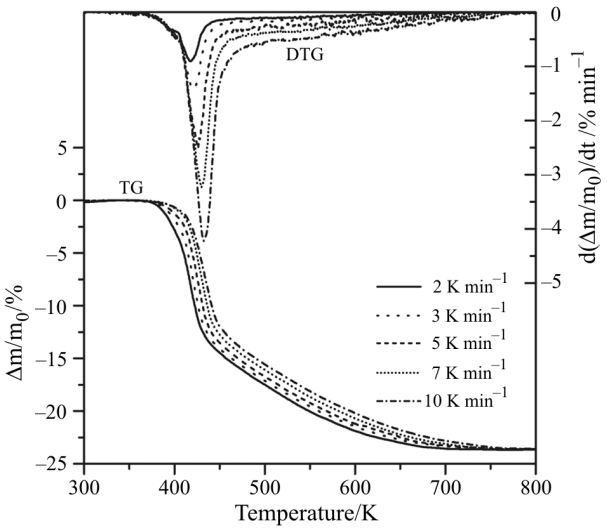

Fig. 5 Typical TG and DTG curves for the thermal dehydration at various heating rates

$K_2B_4O_7{\cdot}4H_2O$. The apparent activation energies, E_a, at various fractional dehydrations, α, were determined by Friedman method [12] known as the isoconversional method in differential form [13, 14]. The α-dependence of E_a for the thermal dehydration process is shown in Fig. 6. Three distinguished ranges of α characterized by different values of E_a, 92.0±19.0 kJ mol^{-1} (α<0.10), 130.3±8.9 kJ mol^{-1} (0.20≤α≤0.4), and 81.3±7.7 kJ mol^{-1} (α>0.6), can be identified. This finding indicates that the thermal dehydration of $K_2B_4O_7{\cdot}4H_2O$ proceeds via, at least, three different kinetic steps. The first kinetic step of the dehydration with E_a=92.0±19.0 kJ mol^{-1} can be distinguished as the surface process proceeds by nucleation and growth. The crack formation takes place as the result of the surface process as observed by SEM, Fig. 3b. The subsequent rapid mass loss process, characterized as the formation process of fine gel powders from sol solution or wet gel produced through an interaction of evolved water vapor and reactant solid, indicates a relatively larger E_a=130.3±8.9 kJ mol^{-1}. The value of E_a decreases in the range 0.4≤α≤0.6 and convergences to 81.3±7.7 kJ mol^{-1} at α>0.6 for the dehydration of aggregated gel powders to form sintered glass.

Subsequent to the glass transition, the as produced anhydrous glass is crystallized via two distinguished exothermic peaks at around 770 and 900 K in DSC curve, Fig. 4. The shape and area of the respective exothermic peaks change systematically depending on the particle size of the sample and the heating rate during the thermal dehydration, Fig. 1. For the as produced glass by the thermal dehydration of the sample of –100+170 mesh at a heating rate of 10 K min^{-1}, the enthalpy changes of the respective crystallization steps were estimated to be –17.6±1.0 and –8.9±1.5 kJ mol^{-1}, respectively. As can be seen from Fig. 3e, a wrinkled surface appears after the first crystallization peak. The cracks produced during the initial dehydration stage of the surface process are still remained in the final crystallization product, triclinic $K_2B_4O_7$, Fig. 3f, indicating a close relationship between the physico-chemical events taking place during the thermal dehydration and kinetic behavior of the crystallization of as produced glass.

Figure 7 shows a comparison of TG-DTA curves for the thermal dehydration of $K_2B_4O_7{\cdot}4H_2O$ annealed for 60 min at various constant temperatures

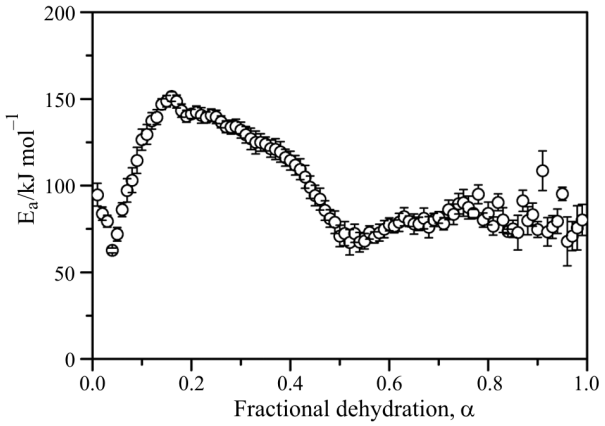

Fig. 6 The α-dependence of E_a determined by Friedman method

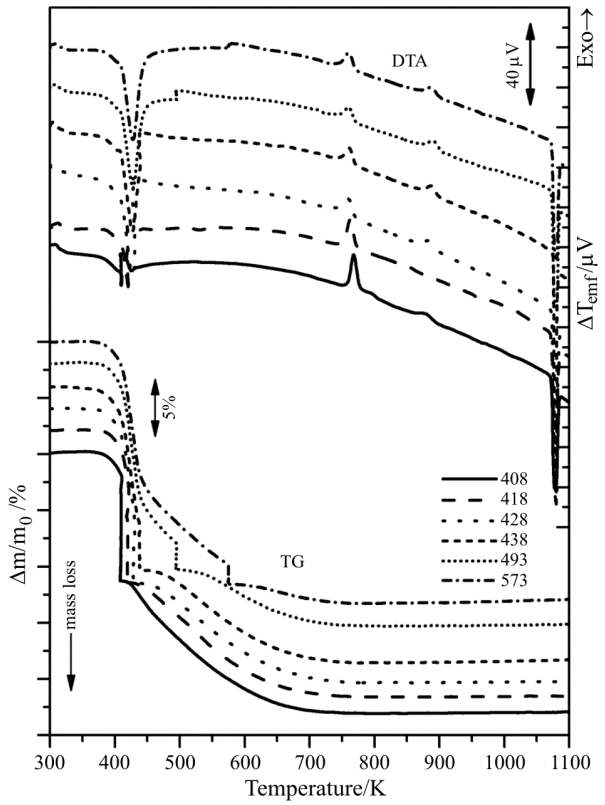

Fig. 7 Comparison of TG-DTA curves annealed at selected temperatures during heating the sample

during heating. The crystallization behaviors of the as produced glass change with the annealed temperature. By annealing at the temperature around the rapid mass loss process of the first half dehydration, the first crystallization exotherm of the as produced glass grows up and the second crystallization exotherm diminishes, whereas the melting temperature of the crystallized $K_2B_4O_7$ remains unchanged. These behaviors indicate that the crystallization behavior of the as produced anhydrous glass can be controlled by regulating the thermal dehydration process.

Detailed kinetic analyses of the thermal dehydration process defined as 'self-induced sol–gel process' and the crystallization of as produced glass via a new intermediate phase will be reported in elsewhere.

Conclusions

The thermal dehydration process of $K_2B_4O_7{\cdot}4H_2O$ was characterized by three distinguished stages of (1) surface process accompanied by the crack formation, (2) rapid mass loss process to form the aggregate of gel powders, and (3) dehydration of gel powders accompanied by sintering. The overall process of the thermal dehydration of $K_2B_4O_7{\cdot}4H_2O$ resembles in mechanism to the glass formation through sol–gel process. The dehydration product was identified as an anhydrous glass, which indicates the glass transition behavior at around 700 K. On further heating the glass crystallizes via two-step processes at around 770 and 900 K.

References

1 A. K. Galwey and M. E. Brown, Thermal decomposition of ionic solids, Elsevier, Amsterdam 1999.
2 A. K. Galwey, Thermochim. Acta, 355 (2000) 181.
3 N. Koga and H. Tanaka, Thermochim. Acta, 388 (2002) 41.
4 M. Touboul and E. Betourne, Solid State Ionics, 63–65 (1993) 340.
5 M. Touboul and E. Betourne, Solid State Ionics, 84 (1996) 189.
6 M. Touboul, N. Penin and G. Nowogrocki, Solid State Sciences, 5 (2003) 1327.
7 N. Koga, J. M. Criado and H. Tanaka, J. Therm. Anal. Cal., 67 (2002) 153.
8 N. Koga, K. Yamaguchi and J. Šesták, J. Therm. Anal. Cal., 56 (1999) 755.
9 N. Koga and J. Šesták, J. Amer. Ceram. Soc., 83 (2000) 1753.
10 J. Krogh-Moe, Acta Crystallograph. B, 28 (1972) 3089.
11 S. Sakka, J. Sol-Gel Sci. Tech., 69–81 (1994).
12 H. L. Friedman, J. Polym. Sci., Part C, 6 (1964) 183.
13 P. Šimon, J. Therm. Anal. Cal., 76 (2004) 123.
14 V. Mamleev, S. Bourbigot, M. Le Bras and J. Lefebvre, J. Therm. Anal. Cal., 78 (2004) 1009.